



OPEN OsPIP2;4 aquaporin water channel primarily expressed in roots of rice mediates both water and nonselective Na⁺ and K⁺ conductance

Sen Thi Huong Tran^{1,3}, Maki Katsuhara¹, Yunosuke Mito², Aya Onishi¹, Ayaka Higa², Shuntaro Ono¹, Newton Chandra Paul^{1,4}, Rie Horie², Yoshihiko Harada² & Tomoaki Horie²✉

Aquaporin (AQP)-dependent water transport across membranes is indispensable in plants. Recent evidence shows that several AQPs, including plasma membrane intrinsic proteins (PIPs), facilitate the electrogenic transport of ions as well as water transport and are referred to as ion-conducting aquaporins (icAQPs). The present study attempted to identify icAQPs that exhibit cation transport activity among PIPs from rice. Electrophysiological experiments on 11 OsPIPs using *Xenopus laevis* oocytes revealed that OsPIP2;4 mediated the electrogenic transport of alkali monovalent cations with the selectivity sequence of Na⁺ ≈ K⁺ > Rb⁺ > Cs⁺ > Li⁺, suggesting non-selective cation conductance for Na⁺ and K⁺. Transcripts of *OsPIP2;4* were abundant in the elongation and mature zones of roots with similar expression levels between the root stelar and remaining outer parts in the cultivar Nipponbare. Immunostaining using sections of the crown roots of Nipponbare plants revealed the expression of OsPIP2;4 in the exodermis and sclerenchyma of the surface region and in the endodermis and pericycle of the stelar region. The present results provide novel insights into OsPIP2;4-dependent non-selective Na⁺ and K⁺ transport and its physiological roles in rice.

Keywords Ion-conducting Aquaporins, Non-selective cation channel, Rice, Roots

Plant aquaporins (AQPs) form a tetrameric membrane channel that facilitates the passive transport of substrates, including water^{1,2}. In higher plants, AQPs are divided into 5 subfamilies: plasma membrane intrinsic proteins (PIPs), tonoplast intrinsic proteins (TIPs), nodulin-26-like intrinsic proteins (NIPs), small basic intrinsic proteins (SIPs), and X intrinsic proteins³. Water uptake from soil and its distribution to all tissues/organs in plants, mediated by AQPs, are vital in plants, and, thus, AQP-dependent water transport plays a key role in controlling essential physiological processes, including cell expansion and stomatal movement⁴. Some AQPs only mediate water transport, while others also mediate the transport of metalloids^{5–7}, gases^{8–12}, and reactive oxygen species^{13,14}. The identification of these novel substrates has broadened the physiological roles of plant AQPs.

In addition to water and neutral solutes, some plant AQPs have been suggested to mediate the transport of ions^{15,16}. In humans, 3 of the 13 AQPs, AQP0, AQP1, and AQP6, have been recognized as dual water and ion channels¹⁷. More recently, AtPIP2;1 and AtPIP2;2 aquaporins from *Arabidopsis* plants, both of which exhibit robust water transport activity, have been shown to mediate non-selective cation conductance in *Xenopus laevis* oocytes, which are deduced to be mainly associated with Na⁺^{18,19}. Furthermore, HvPIP2;8 from barley plants was electrophysiologically characterized as a non-selective cation channel that preferably mediated the transport of Na⁺ and K⁺ when expressed in *X. laevis* oocytes²⁰. Thirty-three AQP genes have been identified in rice (*Oryza sativa* L. cv. Nipponbare), including 11 PIPs, 10 TIPs, 10 NIPs, and 2 SIPs²¹. Six additional AQPs were subsequently found in rice based on the rice genomic sequence²². One of the PIP isoforms in rice,

¹Institute of Plant Science and Resources, Okayama University, 2-20-1 Chuo, Kurashiki, Okayama 710-0046, Japan.

²Division of Applied Biology, Faculty of Textile Science and Technology, Shinshu University, 3-15-1 Tokida, Ueda, Nagano 386-8567, Japan. ³Department of High-Tech agriculture, Faculty of Agronomy, University of Agriculture and Forestry, Hue University, Hue 530000, Vietnam. ⁴Department of Agronomy, Khulna Agricultural University, Khulna 9100, Bangladesh. ✉email: horie@shinshu-u.ac.jp

OsPIP1;3, which was shown to be up-regulated in roots under drought stress, was recently reported to mediate the transport of nitrate anions when expressed in mammalian HEK293 cells, and contributed to water transport when co-expressed with OsPIP2;2 in *X. laevis* oocytes²³. AQP that facilitate the electrogenic transport of cations and anions have been referred to as “ion-conducting AQPs (icAQPs)”²⁴.

In the present study, OsPIPs in rice (OsPIP1;1 to OsPIP1;3 and OsPIP2;1 to OsPIP2;8) were subjected to an electrophysiological survey to search for icAQPs conducting cations, such as Na⁺ and K⁺, in two-electrode voltage clamp (TEVC) experiments using *X. laevis* oocytes. The results obtained herein provide clear evidence to show that OsPIP2;4, an abundantly expressed aquaporin in roots, elicited robust cation conductance and is one of the icAQPs in rice. The present results on the cation selectivity of OsPIP2;4, the investigation of possible hetero-tetramer formation with OsPIP1s, and tissue-specific localization using an anti-OsPIP2;4 peptide antibody provide novel insights into the cation transport function of OsPIP2;4 and its physiological roles as an icAQP under different ionic conditions.

Materials and methods

Plant material and growth conditions

Rice seeds (*O. sativa* L. cv. Nipponbare) were sterilized and germinated as previously described²⁵. Seedlings were hydroponically cultured using a half-strength Kimura B nutrient solution and grown in a growth chamber (LPH-241PFD; NK System, Osaka, Japan) with the settings of a light/dark cycle of 16/8 h and a temperature regimen of 28/25°C.

Preparation of *OsPIP* cRNAs and expression in *X. laevis* oocytes

The coding region of each *OsPIP* cDNA (from cv. Nipponbare) was cloned into the vector pXβG-ev1²⁶. Each construct was linearized and cRNAs were synthesized using the mMACHINE T3 kit (Thermo Fisher Scientific, MA, USA) with a final concentration of 1 μg/μL.

X. laevis frog oocytes were prepared using modified Barth's solution as previously described²⁰. Following the injection of 10 ng of each *OsPIP2* cRNA, 40 ng of each *OsPIP1* cRNA, or water (negative control) into oocytes, they were incubated in MBS at 18 °C for 1 day. Experiments using frog oocytes were approved by the Animal Care and Use Committee, Okayama University (approval number OKU-2017271), which follows the related international and domestic regulations.

Two-electrode voltage clamp (TEVC) experiments using *X. laevis* oocytes

TEVC experiments were performed as previously described^{20,26}. The basic components of bath solutions included 1.8 mM MgCl₂, 1.8 mM Mannitol, 1.8 mM CaCl₂, and 10 mM HEPES, pH 7.5 with Tris (for high Ca) or 1.8 mM MgCl₂, 1.8 mM EGTA (ethylene glycol-bis (β- aminoethyl ether)-N, N, N', N'-tetraacetic acid), 1.8 mM CaCl₂, and 10 mM HEPES, pH 7.5 with Tris (for low Ca: free Ca²⁺ was calculated as 30 μM using <https://somapp.ucdmc.ucdavis.edu/pharmacology/bers/maxchelator/CaMgATPEGTA-NIST-Plot.htm>). The following monovalent cation chloride salts: NaCl, KCl, RbCl, CsCl, or LiCl, were added to the basic solutions for each experiment unless otherwise stated. The osmolality of the bath solutions was adjusted to 200 mosmol Kg⁻¹ with supplemental mannitol. TEVC recordings were performed with an Axoclamp 900 A amplifier and Clampex 9.0 software (Molecular Devices, CA, USA) at room temperature (22–25 °C).

Ion permeability ratios were calculated from the reversal potential shift according to the modified Goldman equation in which the permeability of Cl⁻ was ignored, and only monovalent cations X⁺ (K⁺, Rb⁺, Cs⁺, or Li⁺) and Na⁺ were considered:

$$E_{rev} = -\frac{RT}{F} \ln \left(\frac{P_X [X^+]_{in} + P_{Na} [Na^+]_{in}}{P_X [X^+]_{out} + P_{Na} [Na^+]_{out}} \right)$$

where E_{rev} is the reversal potential (mV); R is the gas constant (8.31 J/K); T is the absolute temperature (Kelvin); F is the Faraday constant (9.654 × 10⁴ C/mol); P_X is the permeability for the ion X⁺; P_{Na} is the permeability for Na⁺; [X⁺]_{out} is the extracellular concentration of X⁺; [X⁺]_{in} is the intracellular concentration of X⁺; [Na⁺]_{out} is the extracellular concentration of Na⁺; [Na⁺]_{in} is the intracellular concentration of Na⁺; RT/F is approximately 25 to 26 mV at the experimental temperature (20 °C).

The intracellular concentrations of ions were not expected to change within a few minutes of the measurements. Therefore, the Goldman equation was modified as follows:

$$\ln \alpha = P_X / P_{Na},$$

$$E_{rev} = -58 \log \left(\frac{\text{Constant}}{\alpha [X^+]_{out} + [Na^+]_{out}} \right) \text{ (mV)}$$

Two reversal potentials, $E_{rev(1)}$ and $E_{rev(2)}$, were measured using two different external solutions with the concentrations of X⁺ and Na⁺ as follows: External solution (1); [X⁺]_{out(1)} and [Na⁺]_{out(1)} for $E_{rev(1)}$; External solution (2); [X⁺]_{out(2)} and [Na⁺]_{out(2)} for $E_{rev(2)}$. According to E_{rev} described above,

$$\begin{aligned}
 E_{rev(1)} - E_{rev(2)} &= -58 \log \left(\frac{Constant}{\alpha [X^+]_{out(1)} + [Na^+]_{out(1)}} \right) \\
 &+ 58 \log \left(\frac{Constant}{\alpha [X^+]_{out(2)} + [Na^+]_{out(2)}} \right) \\
 &= -58 \log \left(\frac{\alpha [X^+]_{out(2)} + [Na^+]_{out(2)}}{\alpha [X^+]_{out(1)} + [Na^+]_{out(1)}} \right) \text{ (mV)}
 \end{aligned}$$

Based on the values of $E_{rev(1)}$, $E_{rev(2)}$, $[X^+]_{out(1)}$, $[Na^+]_{out(1)}$, $[X^+]_{out(2)}$, and $[Na^+]_{out(2)}$, the ion permeability ratios α (P_X/P_{Na}) were calculated.

Water swelling assays using *X. laevis* oocytes

Water channel activity was evaluated using frog oocytes as previously described²⁷. In brief, oocytes injected with *OsPIP2;4* cRNA and/or each *OsPIP1* cRNA or water were transferred from MBS (200 mOsm) to MBS diluted 2-fold (100 mOsm). Osmotic water permeability (P_o) values were calculated based on changes in the cell volume of each oocyte.

Real-time quantitative PCR (q-PCR) analysis

Shoot and root samples of Nipponbare plants grown in hydroponic cultures were collected. To investigate the spatial expression of *OsPIP2;4* in subdivided roots, different segments of roots (0–5, 5–15, and 15–35 mm from the root tips, stelar parts, and remaining outer parts) were collected. These samples were powdered by a mortar and pestle and total RNA was extracted with an RNeasy Plant Mini Kit (Qiagen, Hilden, Germany). cDNA was synthesized using a Rever Tra Ace kit (Toyobo, Osaka, Japan). Primers used to detect transcripts of the *OsPIP2;4* gene were as follows: forward, 5'-ACCTCTCTCAAGCAGCTTAG-3 and reverse, 5'-GACTCGATTGGTTTGC AAGAA -3', which targeted the 5'-UTR region and provided DNA fragments of approximately 50 bp by PCR. The same primer sets were used to detect transcripts of the *OsHKT1;5* and *OsSMT3* genes (internal control) as those in a previous study²⁸. qPCR was performed as previously described²⁶ and the relative expression of the target genes were calculated.

Immunostaining of *OsPIP2;4*

Crown root samples (3 cm from the root tip) of 14-day-old plants were fixed in a 10% (w/v) formaldehyde buffer solution pH 6.9–7.1 (Nacalai, Kyoto, Japan) supplemented with 60 mM sucrose at room temperature for 2 h. Fixed samples were washed 3 times with phosphate-buffered saline (PBS; 140 mM NaCl, 2.7 mM KCl, 1.5 mM KH_2PO_4 , and 8.1 mM Na_2HPO_4 (Nippongene, Tokyo, Japan)) and then embedded in 5% agarose (Takara, Shiga, Japan) with PBS at 4 °C overnight. Micro-sliced samples with a thickness of 100 μ m were prepared with MicroSlicer (Dosaka EM, Kyoto, Japan) and then treated with 0.1% (w/v) pectolyase Y-23 (Kyowa Chemical, Saitama, Japan) in PBS-T (PBS supplemented with 0.3% Tween 20 (Nacalai)) at 30 °C for 2 h in a moisture chamber. After washing with PBS 3 times and blocking with 5% bovine serum albumin (Sigma, USA) in PBS at 30 °C for 10 min, an anti-*OsPIP2;4* rabbit antibody (generated against the synthetic peptide VDVSTLEAGGAR, Eurofins, Kyoto, Japan) was applied to samples (Supplementary Fig. 1). Non-immune rabbit serum was applied as a negative control. Primary antibodies or non-immune sera were reacted at 30 °C overnight. After washing with PBS 5 times, secondary antibodies (an anti-rabbit IgG goat antibody conjugated with Alexa 546 (Thermo Fisher Scientific, MA, USA)) were reacted at 30 °C for another 2 h. After washing with PBS 5 times, samples were analyzed with a confocal laser microscope (FV1000-D, OLYMPUS, Japan).

Data and statistical analyses

Michaelis–Menten curve fitting was performed using Sigma plot 15 software (Hulinks, Tokyo, Japan). A one-way analysis of variance (ANOVA) followed by the least significant difference (LSD) test at the 0.05 level or a one-way ANOVA followed by Duncan's multiple comparisons test was performed. The Students' *t*-test was also used to investigate whether the means of two populations showed a significant difference.

Results

Survey of iAQPs among the PIP subfamily in cultivated rice by TEVC experiments

To conduct an electrophysiological survey of the ion channel activity of each *OsPIP* aquaporin in the presence of large amounts of Na^+ and K^+ , 3 *OsPIP1*s and 8 *OsPIP2*s were expressed in *X. laevis* oocytes. TEVC recordings under a low Ca^{2+} condition (approximately 30 μ M) revealed that only *OsPIP2;4* among all *OsPIP*s tested elicited large inward and outward currents in oocytes in the range of imposed membrane potentials of -120 mV to +30 mV (Fig. 1a, b). Comparisons of ionic conductance also supported that *OsPIP2;4* exhibited the iAQP activity (Fig. 1c). Given that other plant iAQPs such as *AtPIP2;1* and *HvPIP2;8* exhibited strong sensitivity to the external Ca^{2+} ^{18,20}, the effect of an increase in the external Ca^{2+} concentration on the iAQP activity of *OsPIP2;4* was assessed. As a result, no significant difference was found in the *OsPIP2;4*-dependent ionic conductance between low (30 μ M) and high (1.8 mM) Ca^{2+} conditions although high Ca^{2+} tended to slightly reduce the ionic conductance of *OsPIP2;4* ($P=0.146$, one-way ANOVA followed by Tukey HSD post-test; Supplementary Fig. 2). Based on these observations, we decided to adopt 30 μ M as the default Ca^{2+} condition in the bath for the electrophysiological characterization of *OsPIP2;4* unless otherwise stated.

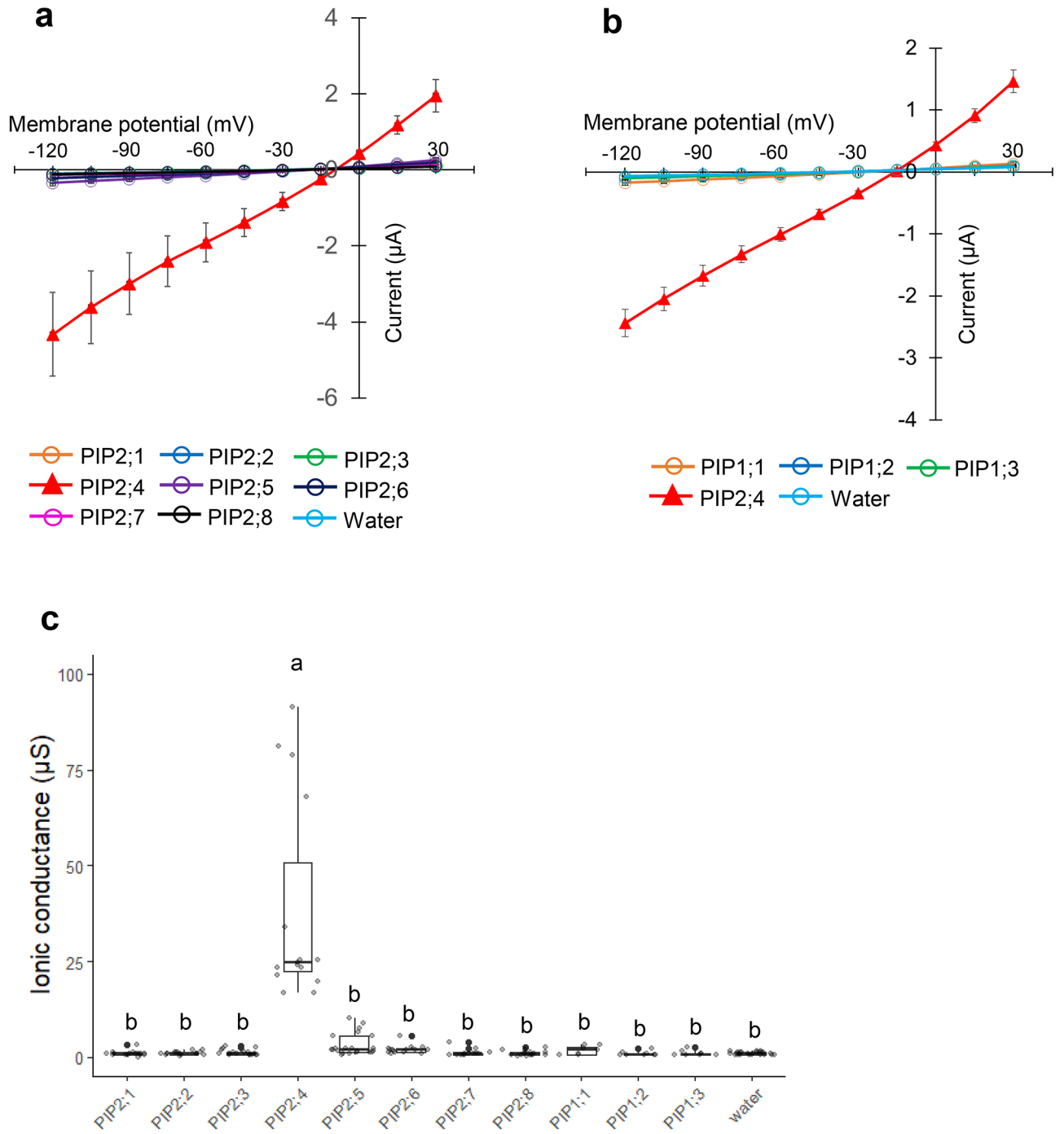


Fig. 1. Electrophysiological survey of the ion-conducting aquaporin (icAQP) on the subfamily of plasma membrane intrinsic proteins in rice (OsPIPs). Two electrode voltage clamp (TEVC) experiments using *X. laevis* oocytes were conducted. **(a)** Current (I)-voltage (V) relationships obtained from oocytes expressing the indicated OsPIP2 proteins or mock water-injected oocytes ($n = 10\text{--}21$). Three independent batches of oocytes were used to obtain these data sets. **(b)** I-V relationships obtained from oocytes expressing the indicated OsPIP1 proteins or mock water-injected oocytes ($n = 5\text{--}8$). OsPIP2;4-mediated currents were also recorded as a positive control ($n = 9$). TEVC recordings were performed in the presence of 86.4 mM NaCl and 9.6 mM KCl with 30 μM Ca^{2+} (for more details, see the Materials and Methods section). A step pulse protocol of -120 mV to $+30$ mV with a 15-mV increment was applied on every oocyte. Data are presented as means \pm SE. **(c)** The ionic conductance calculated from the recordings shown in a and b ($V = -90$ mV to -120 mV). Significant differences ($P < 0.05$) are analyzed using one-way ANOVA followed by Tukey HSD post-test and indicated by different alphabets.

Characteristics of OsPIP2;4 as an ion channel

We investigated the cation and Cl^- dependency of OsPIP2;4-mediated currents in *X. laevis* oocytes. TEVC recordings were conducted using three different bath solutions: 96 mM NaCl, 96 mM Na-gluconate, and 96 mM Choline-Cl. The results obtained clearly showed that Na^+ , but not Cl^- elicited currents in oocytes expressing OsPIP2;4 (Supplementary Fig. 3). Selectivity for alkali cations was subsequently examined. Large inward and outward currents were recorded when OsPIP2;4-expressing oocytes were immersed in a bath solution including 96 mM KCl or 96 mM NaCl (Fig. 2a). The same amount of RbCl and CsCl also elicited OsPIP2;4-mediated currents in a similar manner; however, current amplitudes at the membrane potentials tested were markedly lower than those in NaCl and KCl solutions (Fig. 2a, c). In addition, the presence of 96 mM LiCl evoked weaker

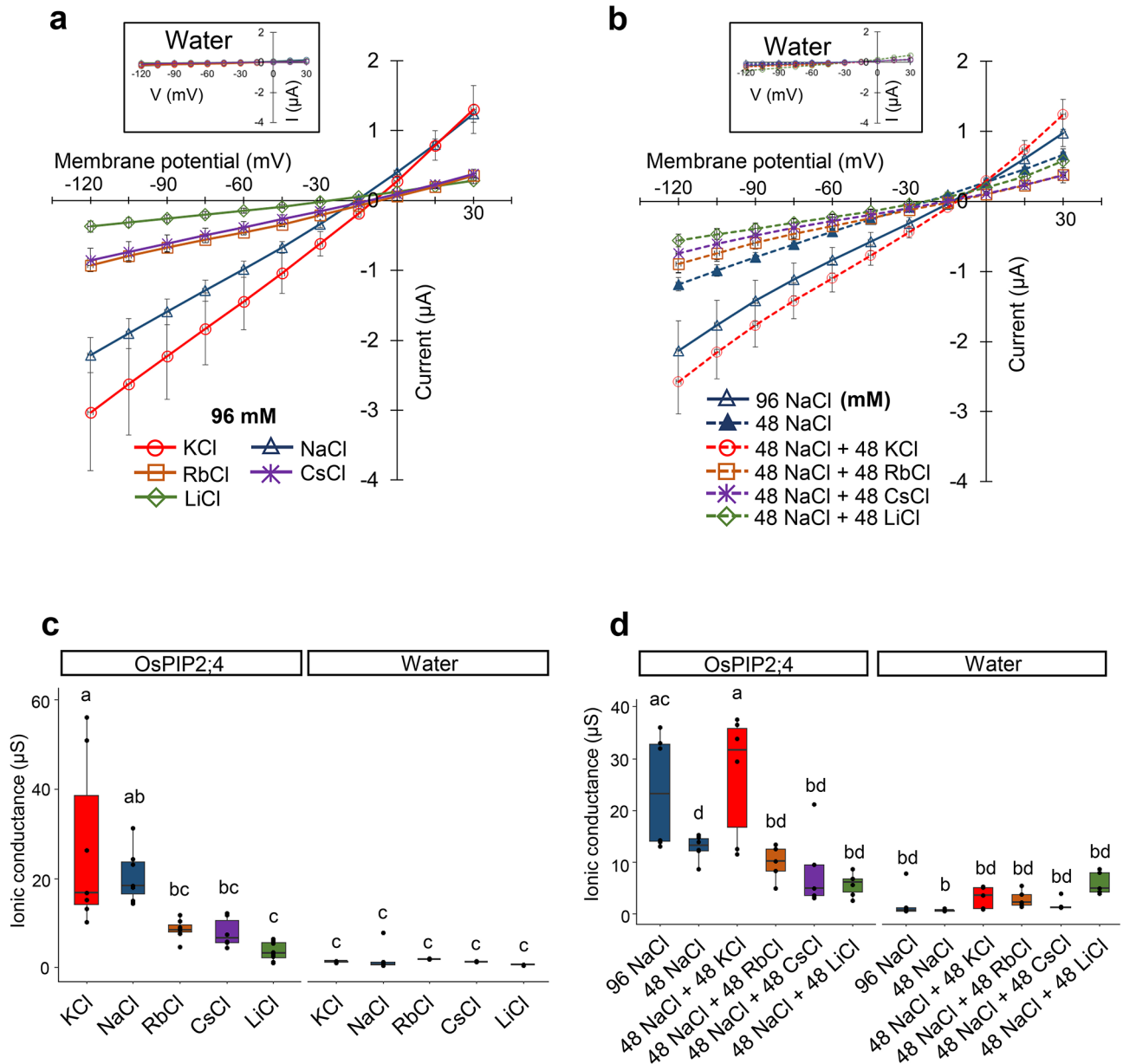


Fig. 2. Monovalent alkaline cation selectivity of OsPIP2;4. TEVC experiments were performed using *X. laevis* oocytes. **(a)** I-V relationships obtained from OsPIP2;4-expressing oocytes ($n=6-8$) or water-injected oocytes ($n=5$; inset) bathed in the solution of a 96 mM monovalent cation chloride salt (K, Na, Rb, Cs, or Li) with $30 \mu\text{M Ca}^{2+}$. **(b)** Effects of the co-presence of a monovalent cation salt with NaCl on OsPIP2;4-mediated ion channel activity. I-V relationships obtained from OsPIP2;4-expressing oocytes ($n=5-6$) or water-injected oocytes ($n=5$; inset) bathed in the solution including 48 mM NaCl, a 48 mM monovalent cation chloride salt, and $30 \mu\text{M Ca}^{2+}$. A step pulse protocol of -120 mV to $+30 \text{ mV}$ with a 15-mV increment was applied on every oocyte. Data are presented as means \pm SE. **(c, d)** The ionic conductance calculated from the recordings shown in a and b, respectively ($V = -90 \text{ mV}$ to -120 mV). Significant differences ($P < 0.05$) are analyzed using one-way ANOVA followed by Tukey HSD post-test and indicated by different alphabets.

inward and outward currents although the statistical analysis on the ionic conductance did not show a significant difference between OsPIP2;4-expressing oocytes and mock water-injected oocytes under the condition (Fig. 2a, c).

Furthermore, OsPIP2;4-mediated currents were recorded in the co-presence of two different monovalent cations: 48 mM Na⁺ and 48 mM X⁺ (where X represents K, Na, Rb, Cs, or Li), added as chloride salts. Smaller currents were observed than those in a 48 mM Na⁺ solution when 48 mM Rb⁺, Cs⁺, or Li⁺ was co-presented (Fig. 2b). In contrast, the addition of 48 mM NaCl or 48 mM KCl to the basic NaCl bath solution markedly enhanced both inward and outward currents, with these increases being dependent on OsPIP2;4 (Fig. 2b, d). In these cases, positive shifts were noted in the reversal potentials (Fig. 2b), indicating that OsPIP2;4 was highly selective for K⁺ and mediated K⁺ transport in the presence of a large amount of Na⁺. These results suggest that among the alkali cations tested, OsPIP2;4 exhibited a preference for the transport of K⁺ and Na⁺.

The reversal potential of OsPIP2;4-expressing oocytes in a 96 mM NaCl (48 mM NaCl + 48 mM NaCl; Fig. 2b) solution was approximately -13 mV. In solutions containing 48 mM NaCl and either 48 mM KCl, CsCl, RbCl, or LiCl, the reversal potentials of OsPIP2;4-expressing oocytes were -12, -16, -15, or -30 mV, respectively. Based on these numbers, the ion permeability ratios of OsPIP2;4 were roughly estimated using the modified Goldman equation as shown in Table 1. The highest P_{ion}/P_{Na} ratio was obtained when K⁺-derived data were applied, and was approximately 1.08, while the lowest ratio was observed for Li⁺ (Table 1).

The features of OsPIP2;4 as a K⁺/Na⁺ channel were further characterized in TEVC experiments. When the amount of KCl in the bath solution was reduced from 96 mM to 12 mM, negative shifts in reversal potentials were observed in OsPIP2;4-expressing oocytes, which again demonstrated that OsPIP2;4 transported K⁺ as a substrate (Fig. 3a). Ionic conductance (μS) at membrane potentials of -75 to -120 mV was calculated at all concentrations tested, and Michaelis-Menten curve fitting was then performed (Fig. 3b). Km and Vmax were 38.5 ± 17.7 mM and 20.6 ± 4.3 μS, respectively. Similar experiments were also conducted for Na⁺. When the concentration of NaCl was reduced from 96 mM to 12 mM, similar negative shifts in reversal potentials as those with changes in the concentration of KCl were observed in OsPIP2;4-expressing oocytes (Fig. 3c). These results provide strong support for OsPIP2;4 mediating the transport of Na⁺. Subsequent calculations of ionic conductance (μS) and Michaelis-Menten curve fitting resulted in Km and Vmax of 28.0 ± 17.2 mM and 18.8 ± 4.4 μS, respectively (Fig. 3d).

Effects of the co-expression of OsPIP2;4 with each OsPIP1 on water and ion transport activities

Some PIP1 and PIP2 channels in plants have been reported to form a heterotetramer, which enhanced the activity of PIP2-mediated water transport^{27,29}. Therefore, we investigated whether the co-expression of OsPIP2;4 and each of the three OsPIP1s showed any significant effects in the transport of water and ions. Water swelling assays using *X. laevis* oocytes revealed that co-expression of OsPIP2;4 and each OsPIP1 did not show notable difference in the P_f when compared to that in oocytes solely expressing OsPIP2;4 (Fig. 4a), suggesting that an OsPIP1-stimulated increase in the water transport activity of OsPIP2;4 was unlikely to occur in rice. Consistent with previous findings, OsPIP1s did not exhibit apparent water channel activity when expressed alone in oocytes (Fig. 4a). The effects of the co-expression of OsPIP1 on the ion channel activity of OsPIP2;4 was then examined by TEVC experiments. When OsPIP2;4 was expressed alone in oocytes, large currents were recorded in the presence of 86.4 mM NaCl and 9.6 mM KCl with membrane potentials ranging from -120 mV to +30 mV (Fig. 4b). On the other hand, all three combinations of the co-expression of OsPIP2;4 with each OsPIP1 resulted in larger inward and outward currents than those in water-injected oocytes; however, the magnitude of these currents was approximately 50% that of OsPIP2;4-expressing oocytes (Fig. 4b). These results indicate that the co-expression of OsPIP1s reduced the icAQP activity of OsPIP2;4.

Expression patterns of the *OsPIP2;4* gene in rice

qPCR analyses were performed to investigate *OsPIP2;4* mRNA levels in rice tissues/organs. Roots and shoots were sampled from approximately 3-week-old plants, prepared by hydroponic culture, for total RNA extraction and first-strand DNA synthesis. The results of the qPCR analysis of *OsPIP2;4* indicated that *OsPIP2;4* was predominantly expressed in the roots of rice (Fig. 5a). We then sectioned the roots of approximately 2-week-old rice into 3 parts: 0–5 mm (dividing zone), 5–15 mm (elongation zone), and 15–35 mm (mature zone) from the root tip. qPCR analyses of first-strand DNA derived from these samples revealed the low expression of *OsPIP2;4* in the root tip region and higher expression in the elongation and mature zones (Fig. 5b). We also attempted to separate the roots of approximately 3-week-old rice plants into two longitudinal sections: the root stele and remaining outer regions. The qPCR analysis of these samples showed similar expression levels of *OsPIP2;4* in both regions (Fig. 5c). To confirm the quality of the longitudinal root sections, we also performed a qPCR analysis using specific primers designated for the detection of *OsHKT1;5*, which encodes a Na⁺ channel that

Ion	Na ⁺	K ⁺	Rb ⁺	Cs ⁺	Li ⁺
P_{ion}/P_{Na}	1	1.08	0.85	0.78	0.03

Table 1. Ion permeability ratios of OsPIP2;4 expressed in *X. laevis* oocytes. Ratios were calculated based on the reversal potential shifts recorded in the solution of 48 mM NaCl + 48 mM XCl (where X represents K, Na, Rb, Cs, or Li) and the modified Goldman equation, in which the permeability of Cl⁻ was ignored (for more details, see the materials and methods section).

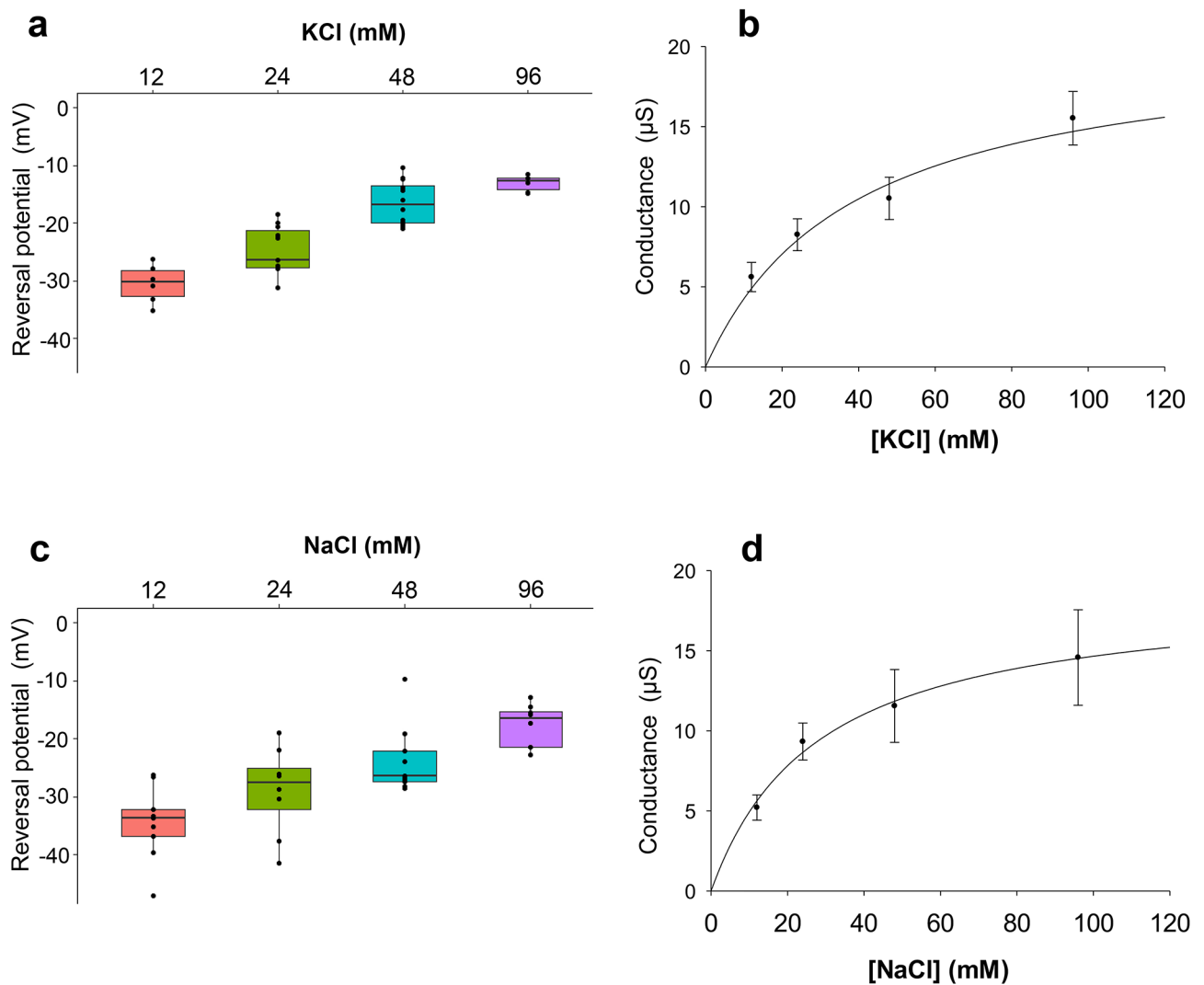


Fig. 3. Characterization of the icAQP activity of OsPIP2;4 in the presence of various concentrations of K^+ and Na^+ . TEVC experiments were performed using *X. laevis* oocytes. (**a**, **c**) Calculated reversal potentials of oocytes expressing OsPIP2;4 in the presence of 12, 24, 48, or 96 mM KCl (**a**) or NaCl (**c**) with $30 \mu M Ca^{2+}$ ($n = 10-12$). A step pulse protocol of -120 mV to $+30$ mV with a 15 -mV increment was applied on every oocyte. (**b**, **d**) An enzyme kinetic analysis of conductance data (μS) at membrane potentials of -75 to -120 mV, obtained from the experiments mentioned in a or c, respectively. Michaelis-Menten curve fitting was performed using Sigma plot software. Two independent batches of oocytes were used for a and b.

has been proven to localize in the vicinity of root xylem²⁸. As shown in Fig. 5d, *OsHKT1;5* was predominantly expressed in the root stele region.

We then investigated the tissue-specific expression of *OsPIP2;4* in the roots of rice. Cross-sections of the roots were prepared from approximately 2-week-old rice plants grown by hydroponic culture. These sections were subsequently used for immunostaining with the anti-OsPIP2;4 peptide antibody. A microscopic analysis of sections visualized with the fluorescent Alexa 546-conjugated anti-rabbit IgG goat antibody led to the detection of major OsPIP2;4-dependent fluorescent signals in the exodermis and sclerenchyma in the outer region of the root and in the endodermis and pericycle of the root stele (Fig. 6d–f). Similar root sectioned samples treated with non-immune rabbit serum did not show apparent fluorescent signals (Fig. 6a–c).

Discussion

Some plant AQPs have been shown to facilitate the transport of ions, in addition to water and/or neutral solutes, and, thus, are called icAQPs²⁴. Based on heterologous expression analyses, icAQP activities were detected or suggested to occur in some plant AQPs derived from wheat¹⁵, soybean¹⁶, grapevine³⁰, *Arabidopsis*^{18,19}, rice²³, and barley²⁰.

In rice, OsPIP1;3 was found to be permeable to NO_3^- , but not HCO_3^-/CO_3^{2-} by a patch-clamping analysis when expressed in mammalian HEK293 cells²³. In the present study, we focused on a survey of icAQPs permeable to monovalent alkali cations (particularly Na^+ and K^+) among OsPIP subfamilies. Electrophysiological TEVC

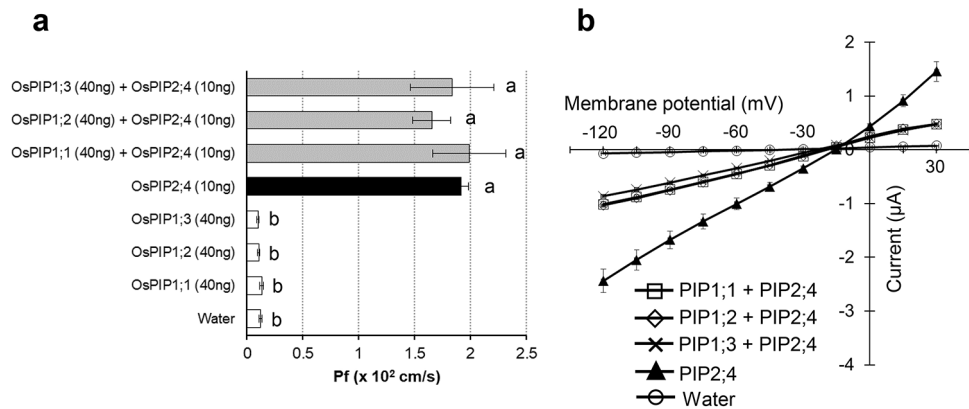


Fig. 4. Effects of OsPIP2;4 co-expression with each OsPIP1 on the transport of water and ions in *X. laevis* oocytes. **(a)** Water swelling assays using oocytes injected with water, 40 ng of each *OsPIP1* cRNA, 10 ng of *OsPIP2;4* cRNA, or 40 ng of each *OsPIP1* cRNA + 10 ng of *OsPIP2;4* cRNA (co-injection) were performed by immersing each oocyte in a hypotonic solution. Significant differences ($P < 0.05$) are indicated by different letters as a result of a one-way ANOVA with Duncan's multiple comparisons test. Data are means \pm SE ($n = 7-10$). P_f represents the water permeability coefficient. **(b)** TEVC analyses using oocytes injected with water, 10 ng of *OsPIP2;4* cRNA, or 40 ng of each *OsPIP1* cRNA + 10 ng of *OsPIP2;4* cRNA (co-injection) were performed. A step pulse protocol of -120 mV to +30 mV with a 15-mV increment was applied on every oocyte in the presence of 86.4 mM NaCl and 9.6 mM KCl with 30 μ M Ca^{2+} . Data are presented as means \pm SE ($n = 5$ for water- and *OsPIP2;4* cRNA-injected oocytes, and $n = 10-11$ for co-injected oocytes).

experiments using *X. laevis* oocytes clearly demonstrated that among the 11 OsPIPs tested, only the OsPIP2;4 protein met the criterion to search for alkali cation permeability (Figs. 1 and 2). OsPIP2;4 exhibited cation channel activity for Na^+ , K^+ , Rb^+ , Cs^+ , and Li^+ in the membrane of *X. laevis* oocytes (Fig. 2). An analysis of ion permeability ratios further suggested the selectivity sequence of OsPIP2;4 of $K^+ \approx Na^+ > Rb^+ > Cs^+$ (Table 1). However, the co-presence of an equal concentration of either Rb^+ , Cs^+ , or Li^+ with Na^+ slightly reduced OsPIP2;4-mediated currents (Fig. 2b), presumably due to competitive inhibition between the substrates. In contrast, the addition of the same amount of K^+ increased OsPIP2;4-mediated currents with positive shifts in reversal potentials, similar to the addition of Na^+ (Fig. 2b). These results strongly suggest that OsPIP2;4 preferably transported Na^+ and K^+ without the competitive substrate inhibition observed in Na^+ versus Rb^+ , Cs^+ , or Li^+ , indicating the non-selective cation channel activity of OsPIP2;4 for Na^+ and K^+ . Together with the ability as a robust water channel (Fig. 4a), these results demonstrated that OsPIP2;4 is an iCAQP that mediates dual water and cation transport.

The structural basis enabling the iCAQPs to transport both water and ions remains to be elucidated. The study of AtPIP2;1 in *Arabidopsis thaliana* led to a mutually exclusive gating hypothesis for water and ion transport, in which the central pore of the channel tetramer is considered to act as an ion-conducting pore²⁴. The hypothesis is supported by the findings that the phosphorylation status in the C-terminal domain of AtPIP2;1 (S280 and S283) has a significant influence on cation transport capacity³¹. A phosphorylation mimic mutant of HvPIP2;8 (S285D), an iCAQP in barley, was shown to facilitate cation transport, which suggested that a similar gating model could be applied to HvPIP2;8 as AtPIP2;1²⁰. The analysis of similar phosphorylation mimic mutants of OsPIP2;4 might gain an insight into the mechanism of dual water and ion transport by iCAQPs.

Previous studies reported Ca^{2+} -sensitive non-selective ionic conductance when AtPIP2;1 and AtPIP2;2 were examined in the presence of a large amount of NaCl (96 mM or 100 mM, respectively) with 2 mM KCl in *X. laevis* oocytes^{18,19}. AtPIP2-mediated ionic conductance, which was presumed to be mainly associated with Na^+ , was also sensitive to external divalent cations, such as Mg^{2+} , Ba^{2+} , and Cd^{2+} ¹⁹. In addition, a recent study demonstrated that one of the PIP2 channels in barley, HvPIP2;8, exhibited similar iCAQP activity when expressed in *X. laevis* oocytes at an external Ca^{2+} concentration of 30 μ M²⁰. HvPIP2;8 also showed strong divalent cation sensitivities to Ca^{2+} , Ba^{2+} , and Cd^{2+} and lower sensitivity to Mg^{2+} ²⁰. The calculated IC_{50} of the HvPIP2;8 channel was approximately 401 μ M of free Ca^{2+} , which was similar to 321 μ M of free Ca^{2+} for AtPIP2;1^{18,20}. In the present study, it was indicated that an increase in the external concentration of Ca^{2+} (from 30 μ M to 1.8 mM) did not lead to a significant difference in the OsPIP2;4-mediated ionic conductance (Supplementary Fig. 2). These results suggest that OsPIP2;4-mediated ionic transport is relatively Ca^{2+} -insensitive and the feature of Ca^{2+} -sensitive ionic conductance might be distinct among plant cation-conducting AQPs. On the other hand, a similar trait for ion channels between OsPIP2;4 and HvPIP2;8 was that both iCAQPs exhibited a preference for Na^+ and K^+ transport independent of Cl^- ²⁰ (Fig. 2, Supplementary Fig. 3). In contrast, AtPIP2;1-mediated cation transport was previously shown to be dependent on Cl^- ¹⁸.

Some plant PIPs affected water transport activity mediated by PIP2 proteins via the formation of heterotetramers²⁷. We investigated whether the co-expression of OsPIP2;4 and each OsPIP1 leads to a significant alteration in the transport of water and cations. Water swelling assays indicated no increase in P_f with the co-expression of OsPIP2;4 with each OsPIP1 (Fig. 4a). However, the same co-expression combinations in TEVC experiments resulted in approximately 60% reductions in ionic conductance from that with the sole expression

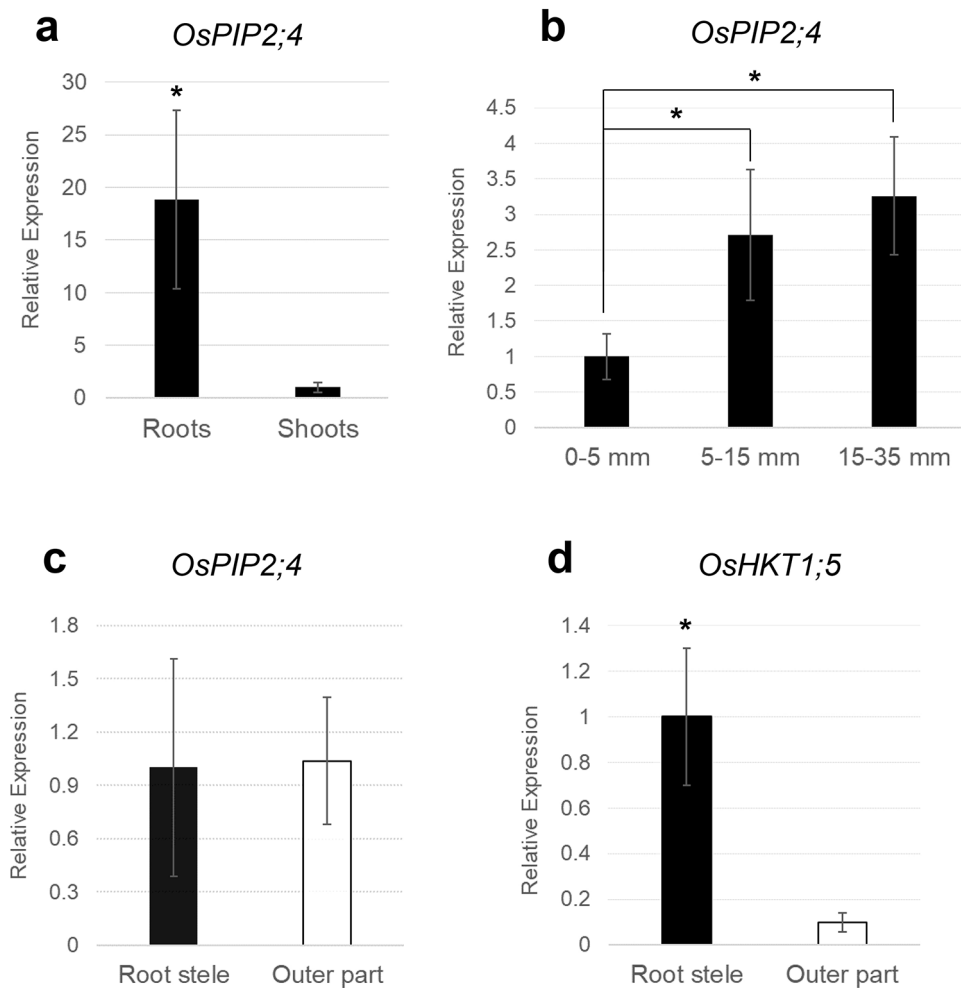


Fig. 5. Real-time PCR analyses of the expression of the *OsPIP2;4* gene in the japonica rice cultivar Nipponbare. **(a)** Root and shoot samples were collected from 3-week-old plants, prepared by hydroponic culture. The relative expression of *OsPIP2;4* is shown with its expression in shoots to 1 ($n = 6 \pm \text{SD}$). **(b)** Roots of 2-week-old rice plants prepared by hydroponic culture were sectioned into 3 parts: approximately 0–5 mm, 5–15 mm, and 15–35 mm from the top of the root. The relative expression of *OsPIP2;4* is shown with its expression in the section 0–5 mm to 1 ($n = 6 \pm \text{SD}$). **(c)** The root stele and remaining outer parts were separated from rice roots, grown by hydroponic culture for 3 weeks. The relative expression of *OsPIP2;4* is shown with its expression in the root stele to 1 ($n = 10–11 \pm \text{SD}$). **(d)** The same root-derived samples as in (c) were used for this experiment. The relative expression of *OsHKT1;5* is shown with its expression in the root stele to 1 ($n = 10 \pm \text{SD}$). The level of target gene expression was normalized by the expression of the *OsSMT3* gene. The Student's *t*-test was performed: * $P < 0.01$.

of *OsPIP2;4* in the presence of 86.4 mM NaCl and 9.6 mM KCl (Fig. 4b). Previous studies reported a similar negative impact on PIP2-mediated cation transport by co-expression with a PIP1 channel in *AtPIP2;1* and *HvPIP2;8*^{18,20}. Further studies are needed to clarify whether this reduction may be attributable to the formation of heteromers and if these phenomena routinely occur in plant cells.

OsPIP2;4 transcripts were mainly detected in the roots of rice, particularly in the elongation and mature zones during the vegetative growth stage (Fig. 5a, b). Moreover, the transcripts accumulated in both the root stele and remaining outer regions in contrast to the root stelar expression of *OsHKT1;5* encoding a Na^+ channel²⁸ (Fig. 5c, d). The results of immunostaining using the anti-*OsPIP2;4* antibody were consistent with those of qPCR analyses, which showed strong *OsPIP2;4*-derived signals in the exodermis and sclerenchyma of the outer part and in the endodermis and pericycle of the stelar part of the rice roots (Fig. 6). Collectively, these results suggest that *OsPIP2;4* contributes to the acquisition of not only water, but also cations from the soil environment to inner cells over the barrier of the Casparian strips in both the exodermis and endodermis of the root³². In terms of plant nutrition, *OsPIP2;4* as a non-selective cation channel appears to play a role in the absorbance and distribution of the essential macronutrient K^+ . Although plants have multiple K^+ transporters^{33,34}, the participation of K^+ -conducting *OsPIP2;4* may provide additional benefits for rice plants for the acquisition of this essential element. However, its putative physiological role needs to be carefully investigated, and more direct evidence is needed. The estimated K_m value for K^+ , based on the data obtained from TEVC experiments, was 38.5 ± 17.7 mM

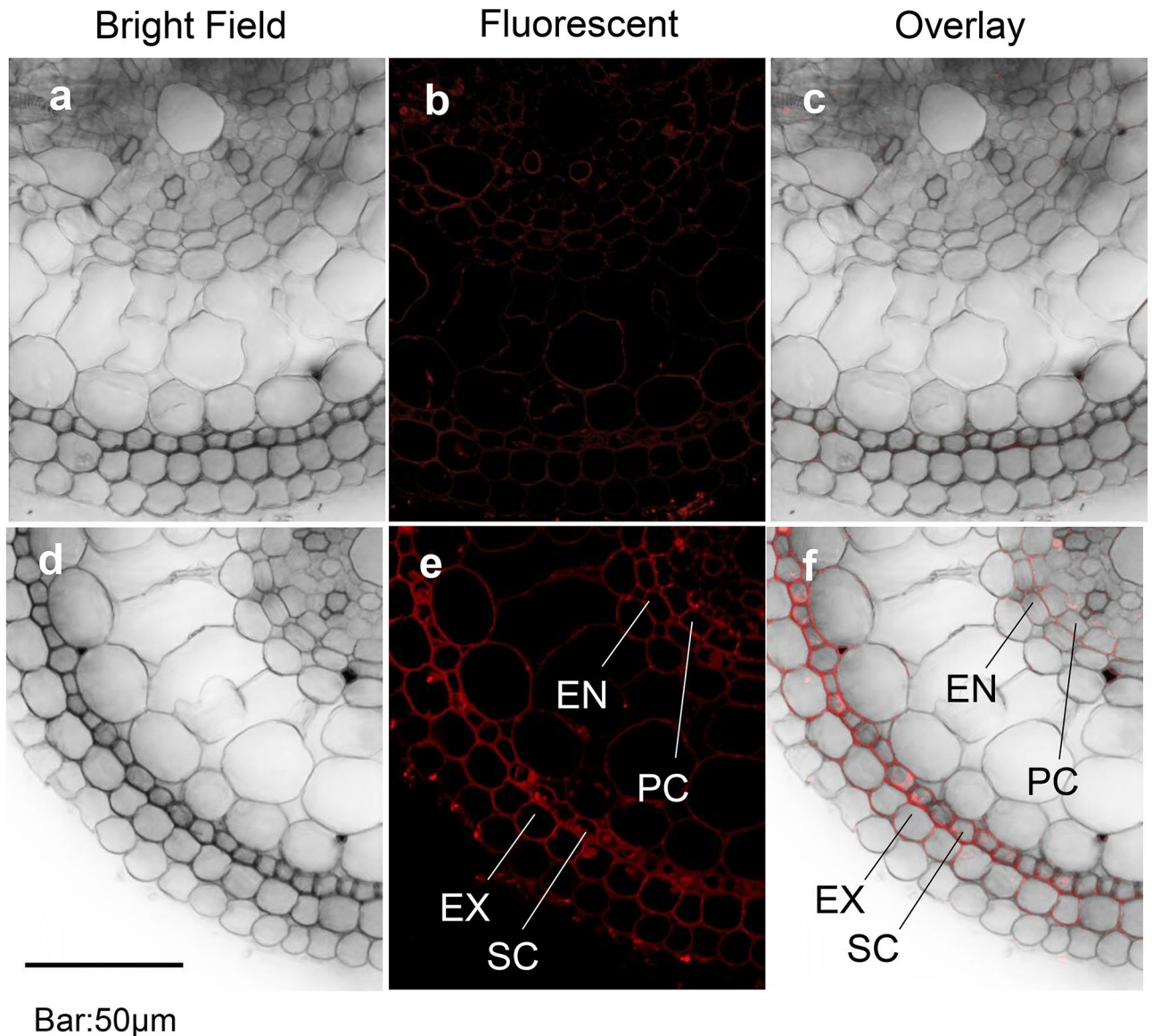


Fig. 6. Tissue-specific localization of OsPIP2;4 in rice crown roots. Cross-sections approximately 30 mm from the root tip were prepared from 2-week-old plants for immunostaining using the anti-OsPIP2;4 peptide antibody. Sections were treated with non-immune rabbit serum (a–c) or hybridized with the anti-OsPIP2;4 rabbit IgG antibody (d–f). Sections were then visualized with a fluorescent Alexa 546-conjugated anti-rabbit IgG goat antibody, and images were obtained with a confocal laser microscope (FV1000-D). Bright field images (a, d), fluorescence images (b, e), and overlaid images (c, f) are shown. Abbreviations in (e, f) were as follows: EX, exodermis; SC, sclerenchyma; EN, endodermis, and PC, pericycle. The bar represents 50 μm .

(Fig. 3a, b). The concentration of available K^+ in soil is generally not high³⁵ and, thus, high-affinity K^+ transport systems are vital for plant nutrition and growth. Regarding the role of OsPIP2;4, it is important to carefully evaluate the contribution of such a low affinity K^+ channel to actual K^+ nutrition in addition to many other K^+ -selective transporters in rice plants. On the other hand, the impact of the Na^+ -conducting nature of OsPIP2;4 needs to be carefully assessed. The estimated K_m value for Na^+ was 28.0 ± 17.2 mM (Fig. 3c, d). If OsPIP2;4 functions as a low affinity Na^+ channel in the surface region of the root (Fig. 6), it may be one of the entries for massive Na^+ influx into plants from saline soil. Furthermore, OsPIP2;4 may facilitate the transport of Na^+ ions over Casparian strips in the exodermis and endodermis, which may have a negative impact on the growth of rice plants under salt stress (Fig. 6). However, OsPIP2;4 may also play a role in Na^+ exclusion from leaves by absorbing Na^+ into cells in the endodermis and pericycle, similar to OsHKT1;5 in rice stellar cells²⁸, providing a positive impact for rice salt tolerance. AtPIP2;1 is one of the most highly expressed aquaporins in the roots of *Arabidopsis* plants³⁶. The Ca^{2+} - and pH-sensitive characteristics of AtPIP2;1-dependent cation transport activity in *X. laevis* oocytes were pointed out to be closely associated with the features of non-selective cation channels in the protoplasts of *Arabidopsis* roots, which have been proposed to facilitate Na^+ influx into *Arabidopsis* roots

during salt stress^{18,37}. Further investigations on several types of *OsPIP2;4* rice mutants, including null, loss-of-ion channel function, and loss-of-water channel function, under various ionic conditions will be crucial for elucidating whether *OsPIP2;4* acts as a dual water and non-selective cation channel in rice plants and clarifying the physiological roles of iCAQPs.

Data availability

The datasets used and/or analyzed during the current study available from the corresponding author on reasonable request.

Received: 23 October 2024; Accepted: 27 March 2025

Published online: 14 April 2025

References

1. Tornroth-Horsefield, S. et al. Structural mechanism of plant aquaporin gating. *Nature* **439**, 688–694 (2006).
2. Verdoucq, L., Rodrigues, O., Martiniere, A., Luu, D. T. & Maurel, C. Plant aquaporins on the move: reversible phosphorylation, lateral motion and cycling. *Curr. Opin. Plant Biol.* **22**, 101–107 (2014).
3. Fox, A. R., Maistriaux, L. C. & Chaumont, F. Toward understanding of the high number of plant aquaporin isoforms and multiple regulation mechanisms. *Plant. Sci.* **264**, 179–187 (2017).
4. Chaumont, F. & Tyerman, S. D. Aquaporins: highly regulated channels controlling plant water relations. *Plant. Physiol.* **164**, 1600–1618 (2014).
5. Kamiya, T. et al. NIP1;1, an aquaporin homolog, determines the arsenite sensitivity of *Arabidopsis Thaliana*. *J. Biol. Chem.* **284**, 2114–2120 (2009).
6. Ma, J. F. et al. A silicon transporter in rice. *Nature* **440**, 688–691 (2006).
7. Takano, J. et al. The *Arabidopsis* major intrinsic protein NIP5;1 is essential for efficient Boron uptake and plant development under Boron limitation. *Plant. Cell.* **18**, 1498–1509 (2006).
8. Dynowski, M., Mayer, M., Moran, O. & Ludewig, U. Molecular determinants of ammonia and Urea conductance in plant aquaporin homologs. *FEBS Lett.* **582**, 2458–2462 (2008).
9. Loque, D., Ludewig, U., Yuan, L. & Wires, N. Tonoplast intrinsic proteins AtTIP2;1 and AtTIP2;3 facilitate NH₃ transport into the vacuole. *Plant. Physiol.* **137**, 671–680 (2005). von.
10. Mori, I. C. et al. CO₂ transport by PIP2 aquaporins of barley. *Plant. Cell. Physiol.* **55**, 251–257 (2014).
11. Uehlein, N., Lovisolio, C., Siefritz, F. & Kaldenhoff, R. The tobacco aquaporin NtAQP1 is a membrane CO₂ pore with physiological functions. *Nature* **425**, 734–737 (2003).
12. Xu, F. et al. Overexpression of rice aquaporin *OsPIP1;2* improves yield by enhancing mesophyll CO₂ conductance and phloem sucrose transport. *J. Exp. Bot.* **70**, 671–681 (2019).
13. Bienert, G. P. & Chaumont, F. Aquaporin-facilitated transmembrane diffusion of hydrogen peroxide. *Biochim. Biophys. Acta.* **1840**, 1596–1604 (2014).
14. Rhee, J., Horie, T., Sasano, S., Nakahara, Y. & Katsuhara, M. Identification of an H₂O₂ permeable PIP aquaporin in barley and a serine residue promoting H₂O₂ transport. *Physiol. Plant.* **159**, 120–128 (2017).
15. Holm, L. M. et al. NH₃ and NH₄⁺ permeability in aquaporin-expressing *Xenopus* oocytes. *Pflugers Arch.* **450**, 415–428 (2005).
16. Weaver, C. D., Shomer, N. H., Louis, C. F. & Roberts, D. M. Nodulin 26, a nodule-specific symbiosome membrane protein from soybean, is an ion channel. *J. Biol. Chem.* **269**, 17858–17862 (1994).
17. Yool, A. J. & Campbell, E. M. Structure, function and translational relevance of aquaporin dual water and ion channels. *Mol. Aspects Med.* **33**, 553–561 (2012).
18. Byrt, C. S. et al. Non-selective cation channel activity of aquaporin AtPIP2;1 regulated by Ca²⁺ and pH. *Plant. Cell. Environ.* **40**, 802–815 (2017).
19. Kourghi, M. et al. Divalent cations regulate the ion conductance properties of diverse classes of aquaporins. *Int. J. Mol. Sci.* **18** (2017).
20. Tran, S. T. H. et al. A survey of barley PIP Aquaporin ionic conductance reveals Ca²⁺-sensitive HvPIP2;8 Na⁺ and K⁺ conductance. *Int. J. Mol. Sci.* **21** (2020).
21. Sakurai, J., Ishikawa, F., Yamaguchi, T., Uemura, M. & Maeshima, M. Identification of 33 rice aquaporin genes and analysis of their expression and function. *Plant. Cell. Physiol.* **46**, 1568–1577 (2005).
22. Bansal, A. & Sankararamkrishnan, R. Homology modeling of major intrinsic proteins in rice, maize and *Arabidopsis*: comparative analysis of transmembrane helix association and aromatic/arginine selectivity filters. *BMC Struct. Biol.* **7**, 27 (2007).
23. Liu, S. et al. Ectopic expression of a rice plasma membrane intrinsic protein (*OsPIP1;3*) promotes plant growth and water uptake. *Plant. J.* **102**, 779–796 (2020).
24. Tyerman, S. D., McGaughey, S. A., Qiu, J., Yool, A. J. & Byrt, C. S. Adaptable and multifunctional ion-conducting aquaporins. *Annu. Rev. Plant Biol.* **72**, 703–736 (2021).
25. Horie, T. et al. Two types of HKT transporters with different properties of Na⁺ and K⁺ transport in *Oryza sativa*. *Plant. J.* **27**, 129–138 (2001).
26. Suzuki, K. et al. *OsHKT1;4*-mediated Na⁺ transport in stems contributes to Na⁺ exclusion from leaf blades of rice at the reproductive growth stage upon salt stress. *BMC Plant Biol.* **16**, 22 (2016).
27. Horie, T. et al. Mechanisms of water transport mediated by PIP aquaporins and their regulation via phosphorylation events under salinity stress in barley roots. *Plant. Cell. Physiol.* **52**, 663–675 (2011).
28. Kobayashi, N. I. et al. *OsHKT1;5* mediates Na⁺ exclusion in the vasculature to protect leaf blades and reproductive tissues from salt toxicity in rice. *Plant. J.* **91**, 657–670 (2017).
29. Jozefkowicz, C., Berny, M. C., Chaumont, F. & Alleva, K. Heteromerization of plant aquaporins. In *Plant Aquaporins: from Transport To Signaling*, (eds Chaumont, F. & Tyerman, S. D.) 29–46 (Springer International Publishing, (2017)).
30. Noronha, H. et al. The grapevine uncharacterized intrinsic protein 1 (VvXIP1) is regulated by drought stress and transports glycerol, hydrogen peroxide, heavy metals but not water. *PLoS One.* **11**, e0160976 (2016).
31. Qiu, J., McGaughey, S. A., Groszmann, M., Tyerman, S. D. & Byrt, C. S. Phosphorylation influences water and ion channel function of AtPIP2;1. *Plant. Cell. Environ.* **43**, 2428–2442 (2020).
32. Kreszies, T., Schreiber, L. & Ranathunge, K. Suberized transport barriers in *Arabidopsis*, barley and rice roots: from the model plant to crop species. *J. Plant. Physiol.* **227**, 75–83 (2018).
33. Gierth, M. & Maser, P. Potassium transporters in plants—involvement in K⁺ acquisition, redistribution and homeostasis. *FEBS Lett.* **581**, 2348–2356 (2007).
34. Maser, P. et al. Phylogenetic relationships within cation transporter families of *Arabidopsis*. *Plant. Physiol.* **126**, 1646–1667 (2001).
35. Sparks, D. L. Bioavailability of soil potassium. In *Handbook of Soil Science*, (ed Sumner, M. E.) D-38-D-52 (CRC, 2000).
36. Alexandersson, E. et al. Whole gene family expression and drought stress regulation of aquaporins. *Plant. Mol. Biol.* **59**, 469–484 (2005).

37. Demidchik, V. & Tester, M. Sodium fluxes through nonselective cation channels in the plasma membrane of protoplasts from Arabidopsis roots. *Plant. Physiol.* **128**, 379–387 (2002).

Acknowledgements

The authors would like to thank Mr. Yoshiyuki Tsuchiya (IPSR, Okayama Univ.) for his technical assistance. We are grateful to the Division of Gene Research, Research Center for Advanced Science and Technology in Shinshu University, for supporting the present study. This work was supported by JSPS KAKENHI Grant Number JP20K06708 to M.K. and T.H., and the Ministry of Education, Culture, Sports, Science and Technology (MEXT) as part of the Joint Research Program implemented at the Institute of Plant Science and Resources, Okayama University in Japan (R415, R515, and R619 to T.H.).

Author contributions

S.T.H.T.: Electrophysiological analysis, Data curation. M.K.: Project administration, Supervision, Electrophysiological analysis, Data curation, Writing—review & editing. Y.M.: Plant culture, qPCR analysis, Data curation. A.O.: Immunostaining, Data curation. A.H.: Plant culture, qPCR analysis. S.O.: Electrophysiological analysis. N.C.P.: Electrophysiological analysis. R.H.: Plant culture, qPCR analysis. Y.H.: qPCR analysis, Data curation.: T.H.: Conceptualization, Electrophysiological analysis, Data curation, Project administration, Supervision, Writing—original draft, Writing—review & editing.

Declarations

Competing interests

The authors declare no competing interests.

Additional information

Supplementary Information The online version contains supplementary material available at <https://doi.org/10.1038/s41598-025-96259-1>.

Correspondence and requests for materials should be addressed to T.H.

Reprints and permissions information is available at www.nature.com/reprints.

Publisher's note Springer Nature remains neutral with regard to jurisdictional claims in published maps and institutional affiliations.

Open Access This article is licensed under a Creative Commons Attribution-NonCommercial-NoDerivatives 4.0 International License, which permits any non-commercial use, sharing, distribution and reproduction in any medium or format, as long as you give appropriate credit to the original author(s) and the source, provide a link to the Creative Commons licence, and indicate if you modified the licensed material. You do not have permission under this licence to share adapted material derived from this article or parts of it. The images or other third party material in this article are included in the article's Creative Commons licence, unless indicated otherwise in a credit line to the material. If material is not included in the article's Creative Commons licence and your intended use is not permitted by statutory regulation or exceeds the permitted use, you will need to obtain permission directly from the copyright holder. To view a copy of this licence, visit <http://creativecommons.org/licenses/by-nc-nd/4.0/>.

© The Author(s) 2025